Blue light does not impair wound healing *in vitro*

Daniela Santos Masson-Meyers, Violet Vakunseh Bumah, Chukuka Samuel Enwemeka *,1

College of Health Sciences, University of Wisconsin-Milwaukee, Milwaukee, WI. USA

ARTICLE INFO

ABSTRACT

Irradiation with red or near infrared light promotes tissue repair, while treatment with blue light is known to be antimicrobial. Consequently, it is thought that infected wounds could benefit more from combined blue and red/infrared light therapy; but there is a concern that blue light may slow healing. We investigated the effect of blue 470 nm light on wound healing, in terms of wound closure, total protein and collagen synthesis, growth factor and cytokines expression, in an *in vitro* scratch wound model. Human dermal fibroblasts were cultured for 48 h until confluent. Then a linear scratch wound was created and irradiated with 3, 5, 10 or 55 J/cm². Control plates were not irradiated. Following 24 h of incubation, cells were fixed and stained for migration and fluorescence analyses and the supernatant collected for quantification of total protein, hydroxyproline, bFGF, IL-6 and IL-10. The results showed that wound closure was similar for groups treated with 3, 5 and 10 J/cm², with a slight improvement with the 5 J/cm² dose, and slower closure with 55 J/cm² $p < 0.001$. Total protein concentration increased after irradiation with 3, 5 and 10 J/cm², reaching statistical significance at 5 J/cm² compared to control ($p < 0.0001$). However, hydroxyproline levels did not differ between groups. Similarly, bFGF and IL-10 concentrations did not differ between groups, but IL-6 concentration decreased progressively as fluence increased ($p < 0.0001$). Fluorescence analysis showed viable cells regardless of irradiation fluence. We conclude that irradiation with blue light at low fluence does not impair *in vitro* wound healing. The significant decrease in IL-6 suggests that 470 nm light is anti-inflammatory.

1. Introduction

It is now well documented that treatment with red or infrared light with less than 200 mW/cm² irradiance and with wavelength in the range of 600 nm to 1000 nm promotes the repair process of skin in experimental animal and human wounds [1–4], ligament [5,6], tendon [7,8], bone [5,9], and cartilage [10,11]. The evidence indicates that red and near infrared light advance tissue repair by enhancing fibroblast migration and proliferation, collagen synthesis [8,12], and by modulating the timing and release of growth factors and cytokines, including basic fibroblast growth factor (bFGF), interleukin 6 (IL-6) and IL-10 [13]. Similarly, accumulating evidence indicates that light between 400 to 480 nm wavelengths, commonly referred to as blue light, is antimicrobial and has been shown to suppress *Staphylococcus aureus*—including methicillin-resistant *S. aureus* [14–21], *Propionibacterium acnes* [22,23],

Pseudomonas aeruginosa [14], *Salmonella enterica* serovars Typhimurium and Heidelberg [24] and other bacteria [23,25–27].

Also, blue light has been shown to improve tissue perfusion by release of nitric oxide (NO) from nitrosyl complexes with hemoglobin in a skin flap model in rats [28]. Since NO formation leads to vasodilatation and subsequent increase in microcirculatory blood flow, the use of blue light might be of great importance for wound healing of diabetic and venous ulcers [29]. Moreover, blue light has been shown to enhance angiogenesis [30] and to be anti-inflammatory [22,31].

These findings suggest that the combination of red/near infrared light and blue light could promote healing and suppress wound infection simultaneously; since red or near infrared light will, as expected, engender faster tissue healing concurrently as infection is kept away with blue light treatment. However, although blue light is well-known to suppress bacterial growth, its potential effect on wound healing remains unknown. The fact that it is antimicrobial suggests that it may suppress tissue repair.

Thus, the purpose of this study was to determine the effect of blue 470 nm light on wound healing, by measuring (1) the rate of wound closure, (2) collagen synthesis, (3) total protein synthesis, (4) growth factor release and (5) cytokines expression, in an *in vitro* scratch model of wound repair. Wounded or scratched, fibroblast monolayers respond to the disruption of cell–cell contacts by secreting more growth factors at the wound margins and promote healing by a combination of proliferation and migration [32–34]. Thus, the scratch assay presents a simple

experimental model of healing in which the cell sheet serves as a surrogate tissue, enabling precise observation of the effect of an experimental intervention [13,32]. The model has been used successfully to reproduce a wound environment *in vitro* and has proven to be a valuable inexpensive tool for gaining initial insight into the effect of experimental treatments on wound healing [35–39]. In this model, the surrogate wound is produced in a monolayer of experimentally cultured fibroblasts, the major cell type in the dermis [38], which promote contractile re-approximation of the wound edges and are vital in synthesizing collagen and other components of the extracellular matrix [40–43].

2. Material and Methods

2.1. Cell Culture

Human dermal fibroblasts isolated from adult skin (Cat. No. C-013-5C) were obtained from Life Technologies Corporation (Carlsbad, CA). Cells were grown in 75 cm^2 cell culture flasks in Dulbecco's modified Eagle's medium (DMEM) supplemented with 10% fetal bovine serum (FBS), 100 U/mL penicillin, and 100 µg/mL streptomycin, in a controlled humidified cell culture incubator (37 °C, 5%CO_2/95% air). The medium was changed every two days. When cells became confluent, the medium was removed, the cell layer was washed with phosphate-buffered saline (PBS) and trypsinized with 0.25% trypsin in buffered ethylenediaminetetraacetic acid (EDTA). Cells were counted in automated cell counter [Cellometer® Auto T4 (Nexcelom Bioscience, Lawrence, MA)] [44]. Prior to the tests, experimental cultures were prepared by seeding cell suspensions at concentrations of 3×10^4 cells/well (1 mL/well) in 24-well microplates and incubated for 48 h in a controlled humidified cell culture incubator to obtain confluent cell growth.

2.2. Scratch Assay

After 48 h of incubation, microplates were observed under an inverted microscope [Olympus® IX51 (Olympus America Inc., Melville, NY)] to confirm the presence of cell growth monolayer. Consistently linear wounds were made using a sterile 5.0 mL pipette tip across the center of each well, creating a cell-free area [35,38,39]. Any cellular debris created from the scratching was removed by gently washing each well twice with DMEM and then 1.0 mL of fresh DMEM (containing 2.5% FBS) was added to each well [45]. The presence of the *in vitro* wound was confirmed under an inverted microscope before plates were irradiated with blue light.

2.3. Light Source and Cell Irradiation

A light-emitting diode (LED) device, the Dynatron Solaris® 708 (Dynatronics Corp., Salt Lake City, UT) fitted with a 470 nm light probe, was used to irradiate the wounded fibroblasts. The applicator, which has a cluster of 32 LEDs, emits blue light with a spectral width of 455–485 nm, and a rating of 150 mW average power and 30 mW/cm^2 irradiance. The light applicator was clamped at a distance of 1–2 mm perpendicularly above each open plate. The device automatically timed the duration of treatment needed per dose [15,16,18–21, 24,44]. As detailed in a previous report, no measurable increase in temperature is generated by the device within the range of fluences used [16]. The fluences used to irradiate the cells were 3, 5, 10 and 55 J/cm^2 based on our previous study [44].

Irradiated groups and non-irradiated controls were subjected to the same environmental conditions in terms of humidity, temperature and time within or outside the incubator, and light–dark cycle. Plated fibroblasts were incubated for 24 h and assayed as summarized in Fig. 1.
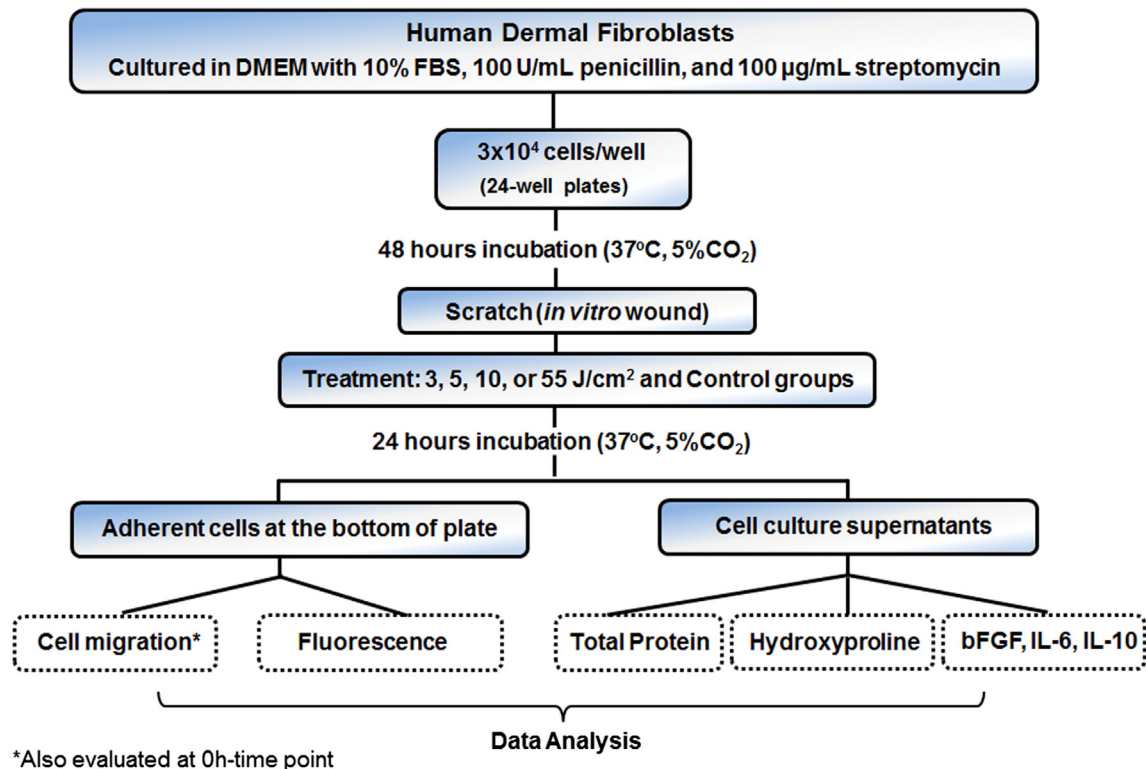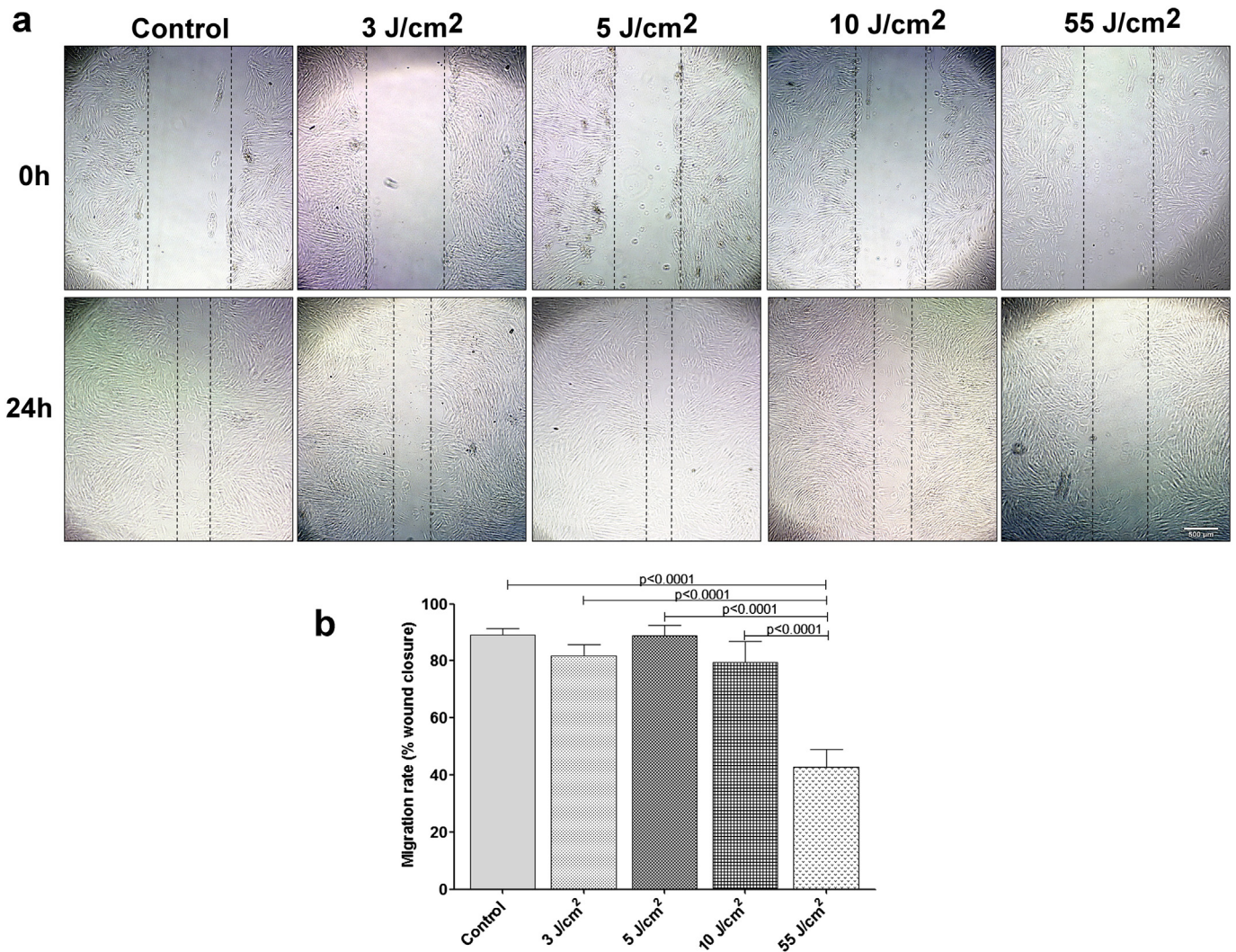

Fig. 1. Experimental design.

Fig. 2. Effects of blue light irradiation on wound closure in the *in vitro* scratch model: (a) Representative photomicrographs of wounded fibroblasts and cell migration at 0 and 24 h after irradiation. The dashed lines indicate the wound edges. Magnification 40×. (b) Quantitative data of the migration rate from 0 to 24 h, expressed in terms of percentage wound closure and presented as mean ± SEM (n = 6).

2.4. Cell Migration/Wound Closure Analysis

To assess cell migration (wound closure/repopulation), images were acquired immediately after wounding (0 hour-time point), and also after irradiation and 24 h of incubation (24 hour-time point), using an inverted microscope (Olympus® IX51 [Olympus America Inc., Melville, NY]) equipped with a digital camera (Olympus® DP70). Cell migration rate (wound closure rate) was determined by comparing the difference between wound width at the zero and the 24 hour time points, using ImageJ software (National Institutes of Health, Bethesda, MD, USA).
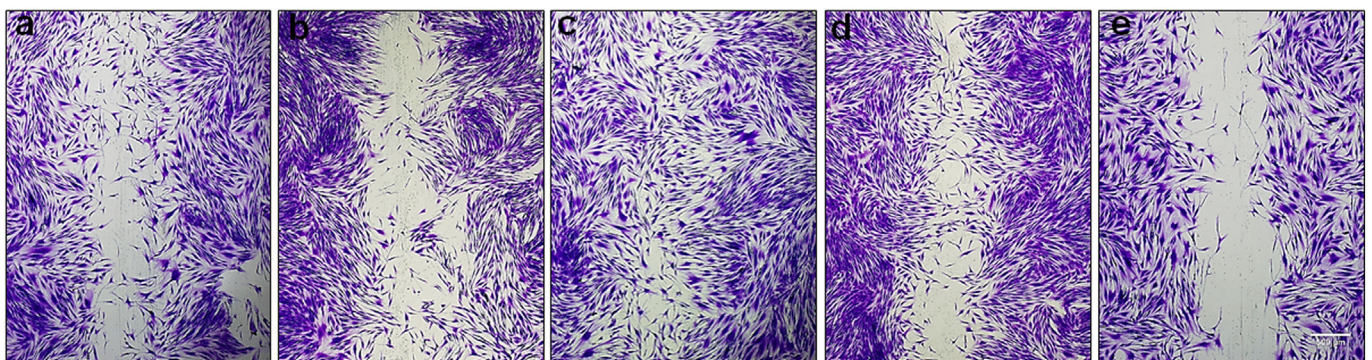

Fig. 3. Representative photomicrographs of wounded fibroblasts stained with crystal violet 24 h after irradiation: (a) Control, non-irradiated cells, (b) 3 J/cm^2, (c) 5 J/cm^2, (d) 10 J/cm^2 and (e) 55 J/cm^2 of 470 nm blue light. Magnification 40×.
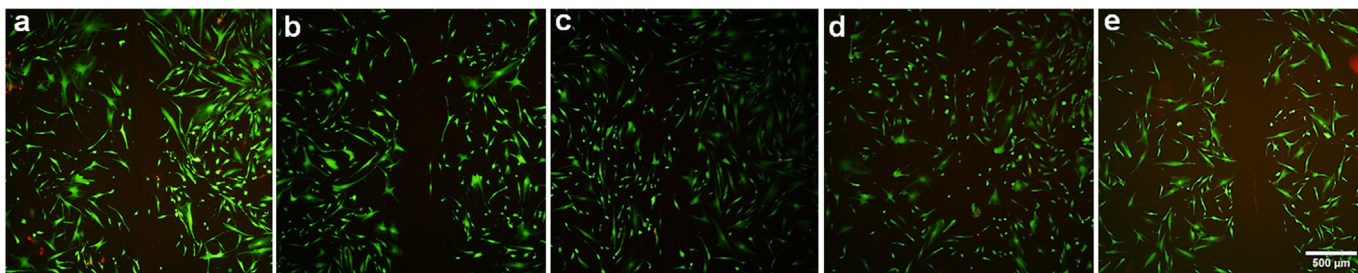
Fig. 4. Representative fluorescent photomicrographs of wounded fibroblasts 24 h after irradiation: (a) Control, non-irradiated cells, (b) 3 J/cm^2, (c) 5 J/cm^2, (d) 10 J/cm^2 and (e) 55 J/cm^2 of 470 nm blue light. Live cells were stained with calcein AM (green fluorescence) and captured using a FITC filter and dead cells were stained with Ethidium homodimer-1 (red fluorescence) and captured using a TRITC filter. Magnification 40×. (For interpretation of the references to color in this figure legend, the reader is referred to the web version of this article.)

Migration rate was expressed as percentage of wound closure using the following equation: $[(At_0 - At_{24}) / At_0] \times 100$, where At_0 is the scratch area at 0 h, and At_{24} is the correspondent scratch area at 24 h [43,46].

Following image acquisition, the supernatants were collected and stored for further assays as detailed below. Then, the surrogate wound (*i.e.*, the adherent fibroblast monolayer) was stained for supplementary data analysis—visualization of migrating/migrated cells. Each well was washed twice with PBS, and cells in each well fixed with 500 μL 4% formaldehyde before incubation at room temperature (RT) for 1 h. Then, 300 μL 0.1% crystal violet was added and plates incubated at RT for 20 min [38]. Wells were then rinsed twice with distilled water and allowed to dry completely before the stained fibroblasts were imaged using an inverted microscope equipped with a digital camera.

2.5. Fluorescence Analysis for Cell Viability/Migration

To further investigate fibroblast migration and viability, wounded fibroblast monolayers were stained with a combination of fluorescent dyes (Ethidium homodimer-1 [EthD-1] and calcein AM) which stain live cells in green and dead cells in red, respectively. Cells were washed once with 500 μL culture-grade PBS. Then 100 μL of fresh PBS plus 100 μL of working solution (4 μM EthD-1; 2 μM calcein AM) was added to each well before incubating the microplates at RT, in the dark for 30–45 min. Plates were then analyzed using an inverted fluorescence microscope (Olympus® IX51) equipped with a digital camera and filters fluorescein isothiocyanate (FITC) with excitation/emission of 480/505–535 nm and tetramethylrhodamine isothiocyanate (TRITC) with excitation/emission of 535/565–610 nm, to permit visualization of live (green) and dead (red) cells, respectively [44]. Two images per replicate were acquired and the results are shown as representative fluorescence photomicrographs.

2.6. Total Protein Assay

A protein assay kit (Quick Start™ Bradford protein assay, Bio-Rad Laboratories, Inc., Hercules, CA) was used to determine protein content in aliquots of cell culture supernatants colorimetrically. The standard curve was determined using bovine gamma globulin at concentrations of 0.125, 0.25, 0.5, 0.75, 1.0, 1.5 and 2.0 mg/mL. Samples were diluted (1:10) in deionized water and a volume of 4.0 μL of each diluted sample and each standard was added to a 96-well microplate, followed by the addition of 200 μL dye reagent [47]. Microplates were then placed in a microplate shaker (Orbit™ P4, Labnet International, Woodbridge, NJ) for 5 min at 20 rpm and the absorbance measured at 595 nm at RT using a multi-detection microplate reader (Synergy™ HT, BioTek Instruments, Inc., Winooski, VT). Absorbance values were plotted against the concentrations of the standards, and the protein concentration in unknown cell supernatants was determined from the standard curve. Tests were done in triplicate and repeated twice (n = 6).

2.7. Hydroxyproline Assay

Hydroxyproline analysis was performed in line with the procedure detailed in previous protocols [39,48,49]. Briefly, 100 μL of cell culture supernatants stored at −20 °C were transferred to a 2.0 mL polypropylene tube. Then, 100 μL of 12 M hydrochloric acid (HCl) was added and samples were hydrolyzed at 120 °C for 3 h. A volume of 20 μL of the hydrolyzed samples was transferred to each well of a 96-well microplate, incubated at 60 °C for 1 h to remove any excess of HCl. Standard solutions of hydroxyproline were prepared at concentrations of 0.2, 0.4, 0.6, 0.8 and 1 μg/mL and added to the plates. Then, a volume of 100 μL/well Chloramine T was added to the samples, standards, blank and plates were incubated at RT for 20 min. A volume of 100 μL/well Ehrlich reagent was added and plates incubated at 60 °C for 20 min. Microplates were homogenized for 10 min at 20 rpm in a microplate shaker and the absorbance measured at 550 nm at RT using a multi-detection microplate reader. Absorbance values were plotted against the concentrations of the standards, and the presence of hydroxyproline in unknown cell supernatants was determined from the standard curve. The amount of hydroxyproline present in the supernatants is an estimate of the collagen content in the scratch wounds, since hydroxyproline is an essential amino acid for collagen synthesis, its content is typically used as a biochemical indicator of the amount of collagen present in a sample [50,51]. Tests were done in triplicate and repeated twice (n = 6).

2.8. Quantification of bFGF, IL-6 and IL-10 Using ELISA

Cell culture supernatants collected and stored at −20 °C were used for these analyses. The concentration of bFGF, IL-6 and IL-10 was assessed with solid phase sandwich ELISA kits (Novex™, Life Technologies Corporation, Carlsbad, CA). Briefly, wells coated with monoclonal antibodies specific for human bFGF, IL-6 or IL-10 were used. The growth factor and cytokines were detected by streptavidin-peroxidase-labeled monoclonal antibody to each target after anti-human biotinylated antibodies were placed in each well and incubated. The wells were washed to remove unbound enzyme-labeled antibodies, then a substrate solution was added, incubated and the reaction was stopped by adding a stop solution. The production of growth factor and cytokines by the wounded fibroblasts was detected as a color change which was read with a multi-detection microplate reader at a wavelength of 450 nm. The intensity of the colored product is directly proportional to the concentration of each growth factor and cytokine present in the samples. Absorbance values were plotted against the concentrations of standards and growth factor and cytokines concentrations in unknown cell supernatants were determined [52–54]. The standard solutions concentrations were 15.6, 31.2, 62.5, 125, 250, 500 and 1000 pg/mL for bFGF and 7.8, 15.6, 31.2, 62.5, 125, 250 and 500 pg/mL for IL-6 and IL-10. Growth factor and cytokines levels were expressed in picograms per milliliter (pg/mL). The kits present sensitivities (minimum detectable

doses) of <15.6 pg/mL (bFGF), <2 pg/mL (IL-6) and <1 pg/mL (IL-10). Tests were done in triplicate and repeated twice (n = 6).

2.9. Statistical Analysis

Quantitative data (cell migration rate, protein, hydroxyproline, bFGF, IL-6 and IL-10) were expressed as mean ± SEM and analyzed using One-way analysis of variance (ANOVA) followed by Bonferroni's post-hoc test (GraphPad Prism 5.01 software, GraphPad Software Inc., USA). The level of statistical difference was set at $p < 0.05$.

3. Results

3.1. Cell Migration and Wound Closure Rate

Monolayers of wounded fibroblasts had clearly demarcated wound margins right after the central scratch was inflicted (Fig. 2a, top panels, 0 h). As shown in Fig. 2a (bottom panels, 24 h), evidence of cell migration across the central scratch can be seen 24 h post-scratching and treatments. Whereas there was no statistical difference in the scratch gap (wound size) of the fibroblasts monolayers irradiated with 3, 5, or 10 J/cm² and controls, the cells irradiated with 55 J/cm² had significantly larger scratch gap when compared to any of the other groups ($p < 0.001$; Fig. 2b), indicating slower wound closure (Fig. 2a, bottom panel and Fig. 2b).

3.2. Cell migration: Crystal Violet Staining

After capturing the 24 hour time point photomicrographs, monolayers of wounded fibroblasts were fixed and stained with crystal violet to enhance the visibility of cell migration as shown in Fig. 3. Similar to the migration results observed with bright field microscopy, irradiation with 5 J/cm² showed more intense cell migration while cells irradiated with 55 J/cm² had larger scratch gap (i.e., exhibited a large cell-free area) compared to the other groups (Fig. 3). These results indicate that the higher fluence (55 J/cm²) of blue light decelerates cell migration in the scratch model, slowing wound closure by fibroblasts in vitro.

3.3. Fluorescence Study of Cell Migration and Viability

Irradiated fibroblasts remained viable at each fluence tested, with each culture showing large amounts of viable cells (green fluorescence) and a few non-viable cells (red fluorescence) (Fig. 4). Consistent with the results obtained from bright field microscopy and crystal violet staining, the outcomes from the fluorescence study show that irradiation with 5 J/cm² resulted in faster migration and repopulation of the scratch wound by fibroblasts while the 55 J/cm² dose slowed repopulation of the scratch gap.

3.4. Total Protein Synthesis

Blue light irradiation moderately advanced protein synthesis at the 3, 10 and 55 J/cm² doses relative to the control group. Irradiation with the 5 J/cm² fluence resulted in a statistically significant increase in total protein synthesis compared to the control group ($p < 0.0001$; Fig. 5).

3.5. Synthesis of Hydroxyproline

Regardless of energy fluence, there was no statistically significant difference in hydroxyproline synthesis between irradiated cells and controls ($p > 0.05$; Fig. 6). This finding may reflect the fact that collagen synthesis does not commence soon after wounding [55,56], even in an in vitro model of wound repair.
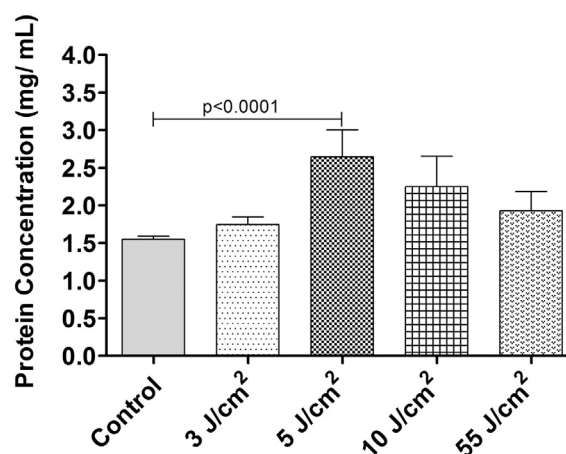

Fig. 5. Effects of blue light on the total protein concentration produced by wounded fibroblasts. Results are presented as mean ± SEM (n = 6).

3.6. Synthesis of bFGF, IL-6 and IL-10

There were no statistically significant differences in the synthesis of bFGF and IL-10 between irradiated cells and controls ($p > 0.05$; Fig. 7a & c). In contrast, following irradiation, there was a statistically significant dose-dependent decrease in IL-6 concentration compared to non-irradiated controls ($p < 0.0001$; Fig. 7b).

4. Discussion

The use of red and near infrared light for wound healing continues to gain popularity and increasing acceptance as accumulating evidence continues to buttress earlier reports that phototherapy speeds wound healing in experimental and clinical settings [3,4,57,58]. Mounting evidence indicates that blue light is antimicrobial [14–26]. This has triggered the notion that simultaneous irradiation of wounds with a combination of red/near infrared light and blue light could yield the dual benefit of faster wound repair and wound disinfection, particularly in infected recalcitrant wounds. The attractiveness of this view is further heightened by reports which indicate that blue light improves tissue perfusion, increases microcirculatory blood flow, enhances angiogenesis and has anti-inflammatory properties [22,28–31]. However, the potential effect of blue light on wound healing remains unknown.

Our findings indicate that irradiation with 470 nm blue light at low fluences of 3, 5 and 10 J/cm² does not adversely affect healing in an
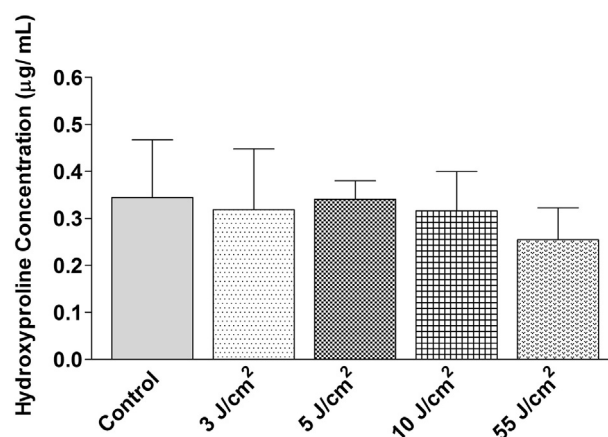

Fig. 6. Effects of blue light on the hydroxyproline levels produced by wounded fibroblasts. Results are presented as mean ± SEM (n = 6).
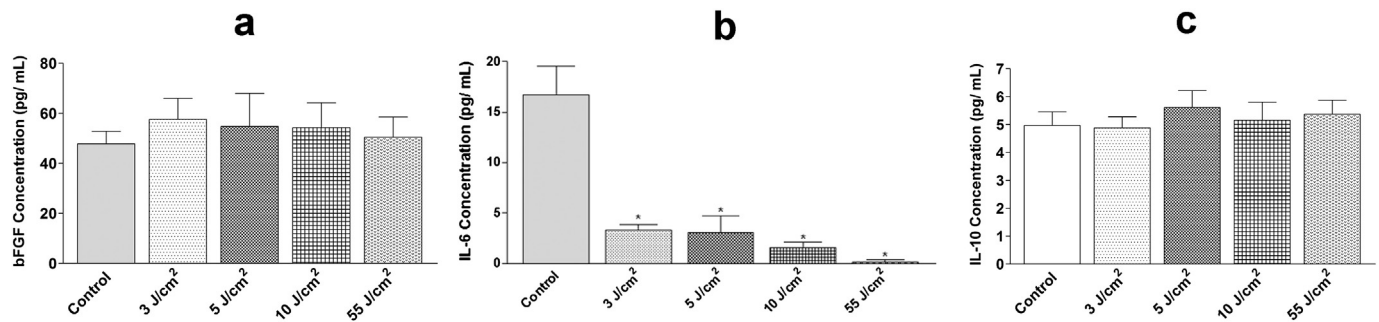
Fig. 7. Effects of blue light on the concentration of: (a) bFGF, (b) IL-6 and (c) IL-10 produced by wounded fibroblasts. Results are presented as mean ± SEM (n = 6). *Represents statistically significant difference between treatment groups and non-irradiated control (p < 0.0001).

in vitro scratch model of wound healing. Whereas our results show that fluences as high as 55 J/cm^2 may slow the rate of wound closure, lower fluences, such as 5 J/cm^2 promote cell migration and faster fibroblast re-population of the scratch wound. Furthermore, fluences in the range of 3 to 10 J/cm^2 significantly diminished IL-6 concentration. The results obtained in our study resonate with previous *in vitro* [59] and *in vivo* [30, 57] investigations on the beneficial effects of blue light in the wound healing process.

Fibroblast migration, proliferation and repopulation of wounds are critical to the successful healing of wounds [38]. Using bright field microscopy, crystal violet staining and fluorescence microscopy, we showed that irradiation doses in the range of 3–10 J/cm^2 do not impair cell migration and wound closure. Indeed, if anything, irradiation at 5 J/cm^2 and to some extent, 10 J/cm^2, appeared to accelerate wound closure. Such improvement was not observed with 55 J/cm^2, which had clear scratch gap that had barely been repopulated with fibroblasts. These findings are consistent with a previous study [59], which indicated that irradiation with 18 J/cm^2 of 405 ± 10 nm had no inhibitory effect on fibroblast function. Similarly, Mamalis et al. [60], have shown that blue light (415 ± 15 nm) irradiation at 30, 45 or 80 J/cm^2 decreased the migration speed of human fibroblasts when compared to untreated controls. Our fluorescence microscopy study confirm our previous report which indicate that control and irradiated fibroblasts remain equally viable, regardless of the irradiation fluence tested [44].

The exposure of wounded fibroblasts to 5 J/cm^2 blue light significantly increased protein synthesis compared to non-irradiated controls. Moderate but statistically insignificant increases were observed at other fluences, particularly at 10 J/cm^2. This finding is significant given the importance of proteins in wound healing and tissue repair, and clinically important if phototherapy was to be administered in the later stages of healing when protein synthesis is highly required [34]. Protein deficiency is well known to impair capillary formation, fibroblast proliferation, proteoglycan synthesis, collagen synthesis, and wound remodeling. Moreover, it can affect the immune system, resulting in a decrease in leukocyte phagocytosis and an increased susceptibility to infection [61]. Conversely, increased protein synthesis is well acknowledged to stem such untoward effects, and herein lies the significance of our finding.

Regardless of dose, the hydroxyproline assay did not reveal any statistically significant difference in synthesis of hydroxyproline between irradiated and non-irradiated fibroblasts. Since this assay is used to estimate collagen synthesis, our finding implies that blue light irradiation did not influence collagen synthesis within 24 h of inducing the scratch wounds *in vitro*. In *in vivo* wound healing, collagen synthesis typically occurs after the initial 3–5 days of injury (*i.e.*, after the inflammation phase of healing) depending of the type of tissue involved [8,55]. It is possible that a similar sequence of healing applies to the *in vitro* scratch wound healing model. In a similar study, Ayuk et al. [56], assessed the collagen content in a diabetic wounded cell model 48 and 72 hour post-irradiation at 660 nm with 5 J/cm^2 and observed a significant increase in collagen production at 72 h compared with 48 h for all experimental groups (irradiated and non-irradiated diabetic wounded fibroblasts, and non-irradiated normal fibroblasts).

Our results indicate that blue light did not affect bFGF expression, neither did it alter the expression of IL-10 relative to controls. However, irradiation significantly decreased IL-6 concentration at each fluence tested. In general, a decrease in the concentration of IL-6, particularly during the inflammatory phase of repair, is considered a positive development since high concentration of IL-6 over a period has the potential to prolong inflammation. This in turn can engender chronic inflammation or inadequate resolution of inflammation, thus creating the type of vicious cycle that perpetuates poor wound healing [40,62]. The dose related decrease in IL-6 concentration following irradiation indicates that blue light has the capacity to stem prolonged inflammation. IL-6 is a pleiotropic pro-inflammatory cytokine expressed and released by a variety of cells including monocytes, macrophages, lymphocytes, and fibroblasts [62,63]. This aspect of our results is consistent with previous reports. Shnitkind et al. [31], have shown similar decreases in inflammatory cytokines IL-1α and ICAM-1 after application of 420 nm light on keratinocytes. Similarly, Kawada et al. [22], reported significant improvement of inflammation in individuals with inflammatory acne following treatment with blue 407–420 nm light.

The results in this study indicate that blue light decreased the level of pro-inflammatory cytokine IL-6 and has the potential to improve wound healing alongside the antimicrobial effects previously reported by our group and others. These findings could possibly expand the application of blue light in wound healing and other inflammatory skin conditions.

5. Conclusion

Our findings suggest that: 1) Irradiation with 470 nm blue light at fluences in the range of 3 to 10 J/cm^2 does not adversely affect healing in an *in vitro* wound model. 2) At 5 J/cm^2 fluence, 470 nm blue light promotes protein synthesis. (3) Regardless of the fluence tested, irradiation with 470 nm light decreases IL-6 concentration in the *in vitro* wound model, indicating that it has the potential to stem prolonged inflammation.

References

[1] M.W. Powell, D.E. Carnegie, T.J. Burke, Reversal of diabetic peripheral neuropathy and new wound incidence: the role of MIRE, Adv. Skin Wound Care 17 (2004) 143–147.

[2] K.S. Caetano, M.A.C. Frade, D.G. Minatel, L.A. Santana, C.S. Enwemeka, Phototherapy improves healing of chronic venous ulcers, Photomed. Laser Surg. 27 (2009) 111–118.

[3] D.G. Minatel, S.C. França, C.S. Enwemeka, M.A.C. Frade, Phototherapy promotes healing of chronic diabetic leg ulcers that failed to respond to other therapies, Lasers Surg. Med. 41 (2009) 433–441.

[4] S.N. Leite, T.A.M. Andrade, D.S. Masson-Meyers, M.N. Leite, C.S. Enwemeka, M.A.C. Frade, Phototherapy promotes healing of cutaneous wounds in undernourished rats, Ann. Bras. Dermatol. 89 (2014) 899–904.

[5] G.A. Guzzarella, P. Torriceli, M. Fini, L. Martini, G. Morrone, R. Giardino, Low-power diode laser stimulation of surgical osteochondral defects. Results after 24 weeks, Artif. Cells Blood Substit. Immobil. Biotechnol. 29 (2001) 235–244.

[6] M. Bayat, A. Delbari, M.A. Almaseyeh, Y. Sadeghi, M. Bayat, F. Reziae, Low-level laser therapy improves early healing of medial collateral ligament injuries in rats, Photomed. Laser Surg. 23 (2005) 556–560.

[7] C.S. Enwemeka, E. Cohen, E.P. Duswalt, D.M. Weber, The biomechanical effects of Ga-As Laser photostimulation on tendon healing, Laser Ther. 6 (1995) 181–188.

[8] G.K. Reddy, L. Stehno-Bittel, C.S. Enwemeka, Laser photostimulation of collagen production in healing rabbit Achilles tendons, Lasers Surg. Med. 22 (1998) 281–287.

[9] G.G.G. Morrone, P. Torriceli, M. Rocca, D. Tigani, G.B. Brodano, M. Fini, R. Giardini, Osteochondral lesion repair of the knee in the rabbit after low-power diode Ga-Al-As laser biostimulation: an experimental study, Artif. Cells Blood Substit. Immobil. Biotechnol. 28 (2000) 321–336.

[10] P.G.G. Torriceli, M. Fini, G.A. Guzzardella, G. Morrone, A. Carpi, R. Giardini, Laser biostimulation of cartilage: in vitro evaluation, Biomed. Pharmacother. 55 (2001) 117–120.

[11] G.A. Guzzarella, P. Porriceli, N.N. Aldini, R. Giardino, Laser technology in orthopedics: preliminary study on low-power laser therapy to improve the bone-biomaterial interface, Int. J. Artif. Organs 24 (2001) 898–902.

[12] G.K. Reddy, L. Stehno-Bittel, C.S. Enwemeka, Matrix remodeling in healing rabbit Achilles tendon, Wound Repair Regen. 7 (1999) 518–527.

[13] D. Hawkins, H. Abrahamse, Effect of multiple exposures of low-level laser therapy on the cellular responses of wounded human skin fibroblasts, Photomed. Laser Surg. 24 (2006) 705–714.

[14] J.S. Guffey, J. Wilborn, Effects of combined 405-nm and 880-nm light on *Staphylococcus aureus* and *Pseudomonas aeruginosa* in vitro, Photomed. Laser Surg. 24 (2006) 680–683.

[15] C.S. Enwemeka, D. Williams, S. Hollosi, D. Yens, S.K. Enwemeka, Visible 405 nm SLD photo-destroys methicillin resistant *Staphylococcus aureus* (MRSA) *in vitro*, Lasers Surg. Med. 40 (2008) 734–737.

[16] C.S. Enwemeka, D. Williams, S. Hollosi, S.K. Enwemeka, S. Hollosi, D. Yens, Blue 470-nm light kills methicillin-resistant *Staphylococcus aureus* (MRSA) *in vitro*, Photomed. Laser Surg. 27 (2009) 221–226.

[17] M. Maclean, K. McKenzie, J.G. Anderson, G. Gettinby, S.J. MacGregor, 405 nm light technology for the inactivation of pathogens and its potential role for environmental disinfection and infection control, J. Hosp. Infect. 88 (2014) 1–11.

[18] V.V. Bumah, D.S. Masson-Meyers, S.E. Cashin, C.S. Enwemeka, Wavelength and bacterial density influence the bactericidal effect of blue light on methicillin-resistant *Staphylococcus aureus* (MRSA), Photomed. Laser Surg. 31 (2013) 547–553.

[19] V.V. Bumah, D.S. Masson-Meyers, S.E. Cashin, C.S. Enwemeka, Optimization of the antimicrobial effect of blue light on methicillin-resistant *Staphylococcus aureus* (MRSA) *in vitro*, Lasers Surg. Med. 47 (2015) 266–272.

[20] V.V. Bumah, D.S. Masson-Meyers, B.J. Quirk, E. Buchmann, H.T. Whelan, C.S. Enwemeka, The bactericidal effect of 470 nm light and hyperbaric oxygen on methicillin-resistant *Staphylococcus aureus* (MRSA), Lasers Med. Sci. 30 (2015) 1153–1159.

[21] D.S. Masson-Meyers, V.V. Bumah, G. Biener, V. Raicu, C.S. Enwemeka, The relative antimicrobial effect of blue 405 nm LED and blue 405 nm laser on methicillin-resistant *Staphylococcus aureus* in vitro, Lasers Med. Sci. 30 (2015) 2265–2271.

[22] A. Kawada, Y. Aragane, H. Kameyama, Y. Sangen, T. Tezuka, Acne phototherapy with a high-intensity, enhanced, narrow-band, blue light source: an open study and in vitro investigation, J. Dermatol. Sci. 30 (2002) 129–135.

[23] T. Dai, A. Gupta, C.K. Murray, M.S. Vrahas, G.P. Tegos, M.R. Hamblin, Blue light for infectious diseases: Propionibacterium acnes, *Helicobacter pylori*, and beyond? Drug Resist. Updat. 15 (2012) 223–236.

[24] V.V. Bumah, D.S. Masson-Meyers, C.S. Enwemeka, Blue 470 nm light suppresses the growth of *Salmonella enterica* and methicillin-resistant *Staphylococcus* (MRSA) *in vitro*, Lasers Surg. Med. 47 (2015) 595–601.

[25] L.E. Murdoch, M. Maclean, E. Endarko, S.J. MacGregor, J.G. Anderson, et al., Sci. World J. (2012), http://dx.doi.org/10.1100/2012/137805.

[26] C.S. Enwemeka, Antimicrobial blue light: an emerging alternative to antibiotics, Photomed. Laser Surg. 31 (2013) 509–511.

[27] Y. Zhang, Y. Zhu, A. Gupta, Y. Huang, C.K. Murray, M.S. Vrahas, M.E. Sherwood, D.G. Baer, M.R. Hamblin, T. Dai, Antimicrobial blue light therapy for multidrug-resistant *Acinetobacter baumannii* infection in a mouse burn model: implications for prophylaxis and treatment of combat-related wound infections, J. Infect. Dis. 209 (2014) 1963–1971.

[28] R. Mittermayr, A. Osipov, C. Piskernik, S. Haindl, P. Dungel, C. Weber, Y.A. Vladimirov, H. Redl, A.V. Kozlov, Blue laser light increases perfusion of a skin flap via release of nitric oxide from hemoglobin, Mol. Med. 13 (2007) 22–29.

[29] R. Ankri, R. Lubart, H. Taitelbaum, Estimation of the optimal wavelengths for laser-induced wound healing, Lasers Surg. Med. 42 (2010) 760–764.

[30] P. Dungel, J. Hartinger, S. Chaudary, P. Slezak, A. Hofmann, T. Hausner, M. Strassl, E. Wintner, H. Redl, R. Mittermayr, Low level light therapy by LED of different wavelength induces angiogenesis and improves ischemic wound healing, Lasers Surg. Med. 46 (2014) 773–780.

[31] E. Shnitkind, E. Yaping, S. Geen, A.R. Shalita, W.L. Lee, Anti-inflammatory properties of narrow-band blue light, J. Drugs Dermatol. 5 (2006) 605–610.

[32] J.C. Yarrow, E.Z. Perlman, N.J. Westwood, T.J. Mitchison, A high-throughput cell migration assay using scratch wound healing, a comparison of image-based readout methods, BMC Biotechnol. 4 (2004), http://dx.doi.org/10.1186/1472-6750-4-21.

[33] U. Terblanche, D.H. Evans, H. Abrahamse, Effect of low level laser therapy on human skin keratinocytes, Med. Tech. SA 23 (2010) 23–29.

[34] P.V. Peplow, T.Y. Chung, C.D. Baxter, Laser photobiomodulation of proliferation of cells in culture: a review of human and animal studies, Photomed. Laser Surg. 28 (2010) S3–S40.

[35] C.C. Liang, A.Y. Park, J.L. Guan, *In vitro* scratch assay: a convenient and inexpensive method for analysis of cell migration in vitro, Nat. Protoc. 2 (2007) 329–333.

[36] D.H. Evans, H. Abrahamse, Efficacy of three different laser wavelengths for in vitro wound healing, Photodermatol. Photoimmunol. Photomed. 24 (2008) 199–210.

[37] M. Fronza, B. Heinzmann, M. Hamburguer, S. Laufer, I. Merfort, Determination of the wound healing effect of calendula extracts using the scratch assay with 3T3 fibroblasts, J. Ethnopharmacol. 126 (2009) 463–467.

[38] F.G. Basso, T.N. Pansani, A.P. Turrioni, V.S. Bagnato, J. Hebling, C.A. de Souza Costa, In vitro wound healing improvement by low-level laser therapy application in cultured gingival fibroblasts, Int. J. Dent. (2012), http://dx.doi.org/10.1155/2012/719452.

[39] M.R. Ab Rahman, F. Abdul Razak, M. Mohd Bakri, Evaluation of wound closure activity of *Nigella sativa*, *Melastoma malabathricum*, *Pluchea indica*, and *Piper sarmentosum* extracts on scratched monolayer of human gingival fibroblasts, Evid. Based Complement. Alternat. Med. (2014), http://dx.doi.org/10.1155/2014/190342.

[40] C.L. Baum, C.J. Arpey, Normal cutaneous wound healing: clinical correlation with cellular and molecular events, Dermatol. Surg. 31 (2005) 674–686.

[41] C. Oplander, S. Hidding, F.B. Werners, M. Born, N. Pallua, C.V. Suschek, Effects of blue light irradiation on human dermal fibroblasts, J. Photochem. Photobiol. 103 (2011) 118–125.

[42] A. King, S. Balaji, L.D. Le, T.M. Crombleholme, S.G. Keswani, Regenerative wound healing: the role of interleukin-10, Adv. Wound Care 3 (2014) 315–323.

[43] F. Felice, Y. Zambito, E. Belardinelli, A. Fabiano, T. Santoni, R. Di Stefano, Effect of different chitosan derivatives on in vitro scratch wound assay: a comparative study, Int. J. Biol. Macromol. 76 (2015) 236–241.

[44] D.S. Masson-Meyers, V.V. Bumah, C.S. Enwemeka, A comparison of four methods of determining viability in human dermal fibroblasts irradiated with blue light, J. Pharmacol. Toxicol. Methods 79 (2016) 15–22.

[45] M.L.Y. Bangaru, S. Chen, J. Woodliff, S. Kansra, Curcumin (diferuloylmethane) induces apoptosis and blocks migration of human medulloblastoma cells, Anticancer Res. 30 (2010) 499–504.

[46] M. Fronza, G.F. Caetano, M.N. Leite, C.S. Bitencourt, F.W.G. Paula-Silva, T.A.M. Andrade, M.A. Frade, I. Merfort, L.H. Faccioli, Hyaluronidase modulates inflammatory response and accelerates the cutaneous wound healing, PLoS ONE 9 (2014), http://dx.doi.org/10.1371/journal.pone.0112297.

[47] Bio-Rad Quick Start™ Bradford protein assay. Instruction manual. Available at: http://www.bio-rad.com/webroot/web/pdf/lsr/literature/4110065A.pdf, accessed on May 20, 2015.

[48] M.P. Jorge, C. Madjarof, A.L. Gois Ruiz, A.T. Fernandes, R.A. Ferreira Rodrigues, I.M. de Oliveira De Sousa, M.A. Foglio, J.E. de Carvalho, Evaluation of wound healing properties of *Arrabidaea chica* Verlot extract, J. Ethnopharmacol. 118 (2008) 361–366.

[49] Sigma-Aldrich. MAK008 Technical bulletin. Available at: http://www.sigmaaldrich.com/content/dam/sigma-aldrich/docs/Sigma/Bulletin/1/mak008bul.pdf, accessed on June 2, 2015.

[50] G.K. Reddy, C.S. Enwemeka, A simplified method for the analysis of hydroxyproline in biological tissues, Clin. Biochem. 29 (1996) 225–229.

[51] J.C. de Oliveira, C.H. de Oliveira, H.E. de Oliveira, G.L. Colombeli, N. De Bona Heck, A. Pereira, A.J. D'Acâmpora, Effects of perioperative hypothermia on healing of anastomosis of the colon in rats, Int. J. Color. Dis. 28 (2013) 705–712.

[52] Novex™ KHG0021 human FGF-basic ELISA kit Protocol. Available at: https://tools.thermofisher.com/content/sfs/manuals/KHG0021_revA8.pdf, accessed on June 15, 2015.

[53] Novex™ KHC0061 human Interleukin-6 (IL-6) ELISA kit Protocol. Available at: https://tools.thermofisher.com/content/sfs/manuals/KHC0061_revB10.pdf, accessed on June 20, 2015. Available at:

[54] Novex™ KHC0101 human Interleukin-10 (IL-10) ELISA kit Protocol. Available at: https://tools.thermofisher.com/content/sfs/manuals/KHC0101_revB6.pdf, accessed on July 1, 2015.

[55] C.S. Enwemeka, Inflammation, cellularity and fibrillogenesis in regenerating tendon: implication for rehabilitation, Phys. Ther. 69 (1989) 816–825.

[56] S.M. Ayuk, N.N. Houreld, H. Abrahamse, Collagen production in diabetic wounded fibroblasts in response to low-intensity laser irradiation at 660 nm, Diabetes Technol. Ther. 14 (2012) 1110–1117.

[57] N. Adamskaya, P. Dungel, R. Mittermayr, J. Hartinger, G. Feichtinger, K. Wassermann, H. Redl, M. van Griensven, Light therapy by blue LED improves wound healing in an excision model in rats, Injury 42 (2011) 917–921.

[58] A. Teuschl, E.R. Balmayor, H. Redl, M. van Griensven, P. Dungel, Phototherapy with LED light modulates healing processes in an in vitro scratch-wound model using 3 different cell types, Dermatol. Surg. 41 (2015) 261–268.

[59] R. McDonald, S.J. Macgregor, J.G. Anderson, M. Maclean, M.H. Grant, Effect of 405-nm high-intensity narrow-spectrum light on fibroblast-populated collagen lattices: an in vitro model of wound healing, J. Biomed. Opt. 16 (2011), http://dx.doi.org/10.1117/1.3561903.

[60] A. Mamalis, M. Garcha, J. Jagdeo, Light emitting diode-generated blue light modulates fibrosis characteristics: fibroblast proliferation, migration speed, and reactive oxygen species generation, Lasers Surg. Med. 47 (2015) 210–215.

[61] S. Guo, L.A. Dipietro, Factors affecting wound healing, J. Dent. Res. 89 (2010) 219–229.

[62] J. Jin, K.P. Sundararaj, D.J. Samuvel, X. Zhang, Y. Li, Z. Lu, M.F. Lopes-Virella, Y. Huang, Different signaling mechanisms regulating IL-6 expression by LPS between gingival fibroblasts and mononuclear cells: seeking the common target, Clin. Immunol. 143 (2012) 188–199.

[63] I. Arranz-Valsero, L. Soriano-Romaní, L. García-Posadas, A. López-García, Y. Diebold, IL-6 as a corneal wound healing mediator in an in vitro scratch assay, Exp. Eye Res. 125 (2014) 183–192.